

Intensity Interferometry for a Chaotic Source with a Collective Flow and Multiple Scattering

Cheuk-Yin Wong*

Physics Division, Oak Ridge National Laboratory, Oak Ridge, TN 37831 USA

(Received December 3, 2017)

Abstract

We study the effects of a collective flow and multiple scattering on two-particle correlation measurements in Hanbury-Brown-Twiss intensity interferometry. We find that under a collective flow the effective source distribution in a two-particle correlation measurement depends on the initial source distribution. In addition, it depends on a collective flow phase function which consists of terms that tend to cancel each other. As the detected particles traverse from the source point to the freeze-out point, they are subject to multiple scattering with medium particles. We examine the effects of multiple scattering on HBT correlations. By using the Glauber theory of multiple scattering at high energies and the optical model at intermediate energies, we find that multiple scattering leads to an absorption and an effective density distribution that depends on the initial source distribution.

PACS numbers: 25.75-q 25.75.Gz 25.75.Ld

*Electronic address: wongc@ornl.gov

I. INTRODUCTION

Intensity interferometry, as first proposed by Hanbury-Brown-Twiss (HBT) to measure the angular diameter of a star using the correlation between two photons [1], has been applied to optical coherence, subatomic physics, and heavy-ion collisions, utilizing different types of particles [2]-[37]. Much information on the space-time distribution of the emitting source is obtained from these measurements.

Recent experimental measurements of HBT correlations in relativistic heavy-ion collisions show only relatively small changes of the extracted longitudinal and transverse radii as a function of collision energies [38, 39, 40, 41, 42, 43]. The small variation of the HBT radii can be explained partly as due to the space-time ordering of the momenta (correlation between the position and the momentum) of the produced particles which was used to explain similar weak collision-energy dependencies of HBT radii in e^+e^- , pp , $p\bar{p}$ collisions (see, for example, Section 17.4 of Ref. [2]). In addition to space-time ordering of momenta, produced particles are subject to collective flows. It is important to find out what physical quantities are measured by the two-particle intensity interferometry for a chaotic source with a collective flow. This will help us understand how collective flows may affect the size parameters extracted in two-particle correlation measurements.

As the detected particles traverse from the source point to the freeze-out point, they are subject to final state mean-field interactions and multiple collisions with particles in the medium. The effect of final mean-field potential has been studied earlier by Gyulassy *et al.* [7]. They found that for a coherent source the only effect of the mean field potential is to redistribute the momentum distribution and the two-particle correlation function is not affected. For a chaotic source, the effect of a mean field is given in terms of distorted wave functions in the mean field [7]. The effects of the mean field in a chaotic source was further studied by Chu *et al.* [26] and Shoppa *et al.* [27]. They found that for low-energy detected particles the Coulomb mean-field leads to substantial modification of the two-particle correlation, but the effect is small for high-energy detected particles.

The collisions of the detected particles with medium particles has been considered to be a source of chaoticity. It is usually assumed that as a result of the random collisions of medium particles, the initial source will evolve into a chaotic source at freeze-out. The source that is observed in HBT measurements will be the chaotic freeze-out source, and the HBT radii will

correspond to those of the freeze-out configuration. For example, in the emission function modeling of [5, 24], an analytical form of the freeze-out phase-space distribution with a collective flow is assumed, and the single-particle distribution and two-particle correlations are described by a freeze-out distribution. In other examples, hydrodynamics or covariant transport theory is followed until freeze-out and the radii of the freeze-out configuration are then extracted to compare with experimental HBT radii [33, 34, 35, 36, 37]. In such an analysis, there is the outstanding puzzle that experimental measurements give $R_{\text{out}}/R_{\text{side}} \approx 0.9 - 1.1$ while hydrodynamical predictions yield $R_{\text{out}}/R_{\text{side}}$ significantly larger than 1.0 at freeze-out [33, 34, 35]. The covariant transport theory can explain the magnitude of R_{out} by assuming a large opacity, but there remains the puzzle that R_{side} is under-estimated [36, 37].

In the context of intensity interferometry, the question whether the freeze-out configuration in a collective flow is a chaotic source needs to be re-examined carefully as the problem of multiple scattering must be treated properly. Because the Hanbury-Brown-Twiss intensity interferometry is purely a quantum-mechanical phenomenon, the problem of multiple scattering must be investigated within a quantum-mechanical framework. We shall focus our attention to high- and intermediate-energy detected particles that have sufficient energies to propagate from the production point to the detection point. It is necessary to study the interference of waves using the probability amplitudes in the multiple scattering process, instead of the conventional description of incoherent collisions in terms of probabilities and cross sections. The Glauber theory of multiple scattering [44] has been shown to be a valid description for the interaction of a pion with the nuclear medium at a pion energy from 300 to 1200 MeV [45, 46, 47]. At lower energies, the optical model [47, 48, 49, 50, 51, 52] has been found to give a very good description of the interaction of a pion with a nucleus from 120 MeV to 766 MeV [50]. They can be applied here to describe the probability amplitudes for the propagation of energetic detected particles (pions from 0.1 to 1 GeV, say). By using the Glauber theory of multiple scattering at high energies and the optical model at intermediate energies, we find that the multiple scattering process leads to an absorption of particles and an HBT effective density distribution that depends on the initial source distribution rather than the freeze-out density distribution.

Previously, the intensity interference was studied in the framework of probability amplitudes for the propagation of produced particles [2]. We shall use the same framework to investigate here the effects of a collective flow and multiple scattering. We examine first the

single-particle distribution in Section II. The probability amplitude for the propagation of a produced particle from the production point to the detected point is obtained. The sum over the probability amplitudes from all the source points then leads to the single-particle distribution which depends on the initial source distribution. In Section III, we study the two-particle momentum distribution. For a chaotic source, the quantum effect of symmetrizing the amplitude for bosons (or anti-symmetrizing the amplitude for fermions) with respect to the exchange of the two particles leads to the phenomenon of intensity interferometry. We show that under a collective flow the two-particle correlation function depends on the initial source distribution and a collective flow phase function. In Section IV, we study the effects of multiple scattering of the detected particles with particles in the medium. In Section V, we discuss the relevance of the present results to HBT measurements in high-energy heavy-ion collisions.

II. SINGLE-PARTICLE DISTRIBUTION

Following arguments similar to those in Ref. [2], we consider the production of a particle with four-momentum $\kappa = (\boldsymbol{\kappa}, \kappa^0)$ at a source point $x = (\boldsymbol{x}, t)$ and its subsequent detection with four-momentum $k = (\boldsymbol{k}, k^0)$ at the space-time point $x_d = (\boldsymbol{x}_d, t_d)$, as shown in Fig. 1. For convenience, we shall use the source center-of-mass system as the reference frame to measure all momenta and space-time coordinates.

To describe the single-particle distribution and intensity interference, we need the probability amplitude for the particle to be produced at the source point x , to propagate to the freeze-out point x_f , and to arrive at the detection point x_d . We can characterize the production probability amplitude for producing a particle of momentum κ at x by a magnitude $A(\kappa x)$ and a phase $\phi_0(x)$. Without loss of generality, the functions $A(\kappa x)$ and $\phi_0(x)$ can be taken to be real, and $A(\kappa x)$ can be taken to be non-negative. The magnitude $A(\kappa x)$ is related to the initial phase-space distribution $f_{\text{init}}(\kappa(x), x)$ (see Eq. (15) below). The production phase $\phi_0(x)$ describes the degree of coherence or chaoticity of the particle production process. We shall be interested in an initially chaotic source which can be represented by random and fluctuating production phases $\phi_0(x)$ at the source points.

The complete probability amplitude $\Psi(\kappa x \rightarrow k x_d)$ for a particle of momentum κ to be produced from the source point x , to propagate along the classical trajectory, and to arrive

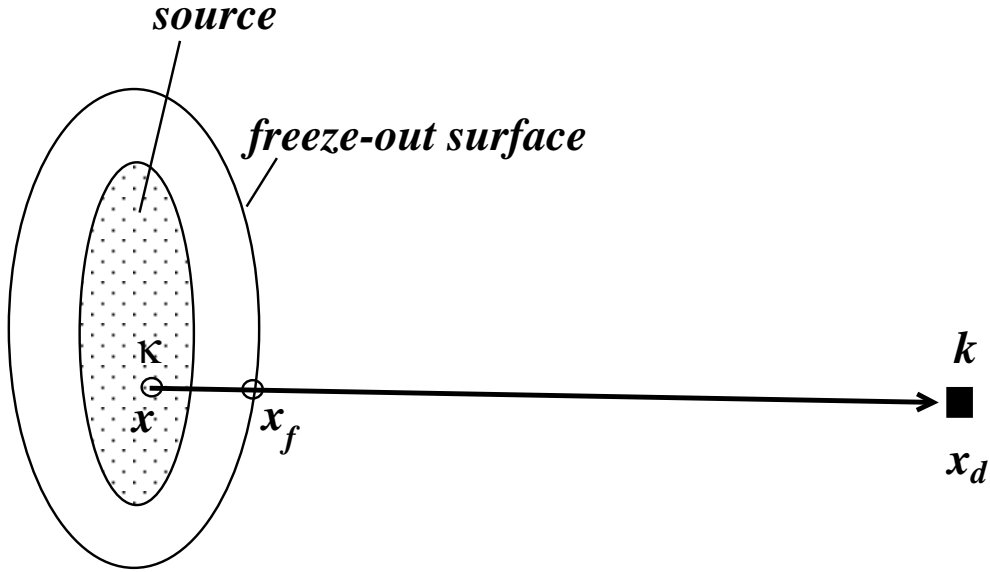


FIG. 1: A particle of momentum κ is emitted at a typical source point x of an extended source, is subject to a collective flow to reach the freeze-out surface at x_f , and is detected with momentum k at the detection point x_d . The straight line joining x to x_d is the trajectory of the particle from x to x_d . The figure is not drawn to scale. The distance between x and x_d is many orders of magnitude greater than the linear dimension of the extended source.

at x_d with momentum k is

$$\Psi(\kappa x \rightarrow k x_d) = A(\kappa x) e^{i\phi_0(x)} \psi(\kappa x \rightarrow k x_d), \quad (1)$$

where $\psi(\kappa x \rightarrow k x_d)$ is the probability amplitude for the propagation of the produced particle from the production point x to the freeze-out point x_f and the detection point x_d . From the path-integral method, this amplitude is given by [2]

$$\psi(\kappa x \rightarrow k x_d) = S(\text{classical path}, \kappa x \rightarrow k x_d) = \exp\left\{-i \int_x^{x_d} \kappa(x') \cdot dx'\right\}, \quad (2)$$

where the integration is carried out along the classical trajectory, and we have used the notation $\kappa(x')$ to represent the momentum of the particle at the space-time point $x' = (\mathbf{x}'t')$ with $t \leq t' \leq t_d$. We consider a Lagrangian picture of collective motion in which we follow the fluid element at x' and its velocity field $\beta(x')$. For a given detected particle with momentum $k = (k^0, \mathbf{k})$, the initial momentum κ depends on the collective flow velocity $\beta(x_f)$ at freeze-out (see Eqs. (3), (4), and (5) below). The freeze-out coordinate x_f in turn depends on the initial source coordinate x . Therefore, $\kappa(x)$ is a function of the initial source coordinate x .

The momentum of the produced particle $\kappa(x')$ in different space-time regions along the classical path from x to x_d is given in the non-relativistic case by:

$$\kappa(x') = \begin{cases} \kappa(x) + m\boldsymbol{\beta}(x'), & \text{for } t \leq t' \leq t_f, \\ \kappa(x) + m\boldsymbol{\beta}(x_f) = \mathbf{k}, & \text{for } t_f \leq t' \leq t_d, \end{cases} \quad (3)$$

and

$$\kappa^0(x') = \begin{cases} [\kappa(x) + m\boldsymbol{\beta}(x')]^2/2m, & \text{for } t \leq t' \leq t_f, \\ [\kappa(x) + m\boldsymbol{\beta}(x_f)]^2/2m = k^0, & \text{for } t_f \leq t' \leq t_d. \end{cases} \quad (4)$$

In the relativistic case, the momentum $\kappa(x')$ under a collective flow with velocity $\boldsymbol{\beta}(x')$ is given by

$$\kappa(x') = \begin{cases} \Lambda(\boldsymbol{\beta}(x'))\kappa(x), & \text{for } t \leq t' \leq t_f, \\ \Lambda(\boldsymbol{\beta}(x_f))\kappa(x) = k, & \text{for } t_f \leq t' \leq t_d, \end{cases} \quad (5)$$

where $\Lambda(\boldsymbol{\beta}(x'))$ is a matrix with elements

$$\begin{aligned} \Lambda_0^0(\boldsymbol{\beta}) &= \gamma = 1/\sqrt{1 - |\boldsymbol{\beta}|^2}, \\ \Lambda_0^i(\boldsymbol{\beta}) &= \Lambda_i^0(\boldsymbol{\beta}) = \gamma\beta^i, \\ \Lambda_k^i(\boldsymbol{\beta}) &= \delta_k^i + \frac{\gamma - 1}{\beta^2}\beta^i\beta^k, \end{aligned} \quad (6)$$

and $i, k = 1, 2, 3$.

The momentum of the particle does not change after freezing out at $t' = t_f$. Thus, the exponential function in $\psi(\kappa x \rightarrow kx_d)$ can be separated into the contribution from x to x_f and from x_f to x_d ,

$$\psi(\kappa x \rightarrow kx_d) = \exp\left\{-i \int_x^{x_f} \kappa(x') \cdot dx' - ik \cdot (x_d - x_f)\right\}. \quad (7)$$

In addition the production from the source point x , the particle can also be produced from other source points in the extended source. The total amplitude for the detection of a particle at x_d is the sum of the probability amplitudes from all source points. After taking into account the production probability amplitude $Ae^{i\phi}$ at different source points, the total probability amplitude for a particle with momentum k to be produced from the extended source and to arrive at the detection point x_d is given by

$$\begin{aligned} \Psi(k : \{\text{all } x \text{ points}\} \rightarrow x_d) &= \sum_x A(\kappa(x), x) e^{i\phi_0(x)} \psi(\kappa x \rightarrow kx_d) \\ &= \sum_x A(\kappa(x), x) e^{i\phi_0(x)} \exp\left\{-i \int_x^{x_f} \kappa(x') \cdot dx' - ik \cdot (x_d - x_f)\right\}. \end{aligned} \quad (8)$$

The single-particle momentum distribution, $P(k)$, which is the probability for a particle of momentum κ to be produced from the extended source and to arrive at the detection point x_d with momentum k , is the absolute square of the total probability amplitude,

$$\begin{aligned} P(k) &= |\Psi(k : \{\text{all } x \}_{\text{points}} \rightarrow x_d)|^2 \\ &= \left| \sum_x A(\kappa(x), x) e^{i\phi_0(x)} \exp\left\{-i \int_x^{x_f} \kappa(x') \cdot dx' - ik \cdot (x_d - x_f)\right\} \right|^2. \end{aligned} \quad (9)$$

We expand the righthand side of Eq. (9) into terms independent of $\phi_0(x)$ and terms containing $\phi_0(x)$. We obtain

$$\begin{aligned} P(k) &= \sum_x A^2(\kappa(x), x) + \sum_{\substack{x, y \\ x \neq y}} A(\kappa(x), x) A(\kappa(y), y) e^{i\phi_0(x)} e^{-i\phi_0(y)} e^{-ik \cdot (x_d - x_f) + ik \cdot (y_d - y_f)} \\ &\quad \times \exp\left\{-i \int_x^{x_f} \kappa(x') \cdot dx' + i \int_y^{y_f} \kappa(y') dy'\right\}. \end{aligned} \quad (10)$$

For an initially chaotic source, the phases at different source points can be described by a random and fluctuating phase $\phi_0(x)$ with a period much shorter than the mean-life of the source. For such a source, the second term on the righthand side of the above equation gives a zero contribution because the large number of terms with slowly varying magnitudes, but rapidly fluctuating random phases, cancel out one another in the sum over the source time coordinate (see Supplement 17.1 of Ref. [2]). The properties and the validity of using the time average for a chaotic source have been discussed in detail in Chapter X of the text of Born and Wolf [53]. Therefore, Eq. (10) becomes

$$P(k) = \sum_x A^2(\kappa(x), x). \quad (11)$$

The summation over the source points necessitates the specification of the initial density $\rho(x)$ of the source points per unit space-time volume at the point x . With this specification, the summation should be transcribed as an integral over x ,

$$\sum_x \dots \rightarrow \int d^4x \rho(x) \dots \quad (12)$$

Therefore, we can rewrite Eq. (11) as

$$P(k) = \int d^4x \rho(x) A^2(\kappa(x), x), \quad (13)$$

which is independent of x_d . We can compare this equation with the properties of the phase space distribution function. One can describe the observed particles as coming from the

initial phase space distribution $f_{\text{init}}(\kappa(x), x)$ defined by

$$P(k) = \int d^4x f_{\text{init}}(\kappa(x), x). \quad (14)$$

A comparison of the above equation with Eq. (13) shows that the observed particle with momentum k comes from the initial phase space distribution

$$f_{\text{init}}(\kappa(x), x) = \rho(x)A^2(\kappa(x), x). \quad (15)$$

One can alternatively describe the observed particles as coming from the freeze-out phase space distribution $f_f(k, x_f)$ defined by

$$P(k) = \int d^4x_f f_f(k, x_f) = \int d^4x f_{\text{init}}(\kappa(x), x). \quad (16)$$

The initial distribution and the freeze-out distribution are equivalent descriptions and they are related to each other by

$$f_f(k, x_f) = \left| \frac{\partial(\mathbf{x}, x^0)}{\partial(\mathbf{x}_f, x_f^0)} \right| f_{\text{init}}(\kappa(x), x) = \left| \frac{\partial(\mathbf{x}, x^0)}{\partial(\mathbf{x}_f, x_f^0)} \right| \rho(x)A^2(\kappa(x), x), \quad (17)$$

where $\left| \partial(\mathbf{x}, x^0)/\partial(\mathbf{x}_f, x_f^0) \right|$ is the Jacobian determinant arising from the mapping of the initial source point $\{\mathbf{x}, x^0\}$ to the freeze-out point $\{\mathbf{x}_f, x_f^0\}$ due to the collective flow.

III. TWO-PARTICLE DISTRIBUTION

We consider the case in which a particle of momentum $\kappa_1(x_1)$ starts from x_1 , propagates to the freeze-out point x_{f1} , and arrives at the detection point x_{d1} with momentum k_1 , and another identical particle of momentum $\kappa_2(x_2)$ starts from x_2 , propagates to the freeze-out point x_{f2} , and arrives at x_{d2} with momentum k_2 , as indicated by the solid lines in Fig. 2. The probability amplitude for the production of the particle with momentum $\kappa_j(x_i)$ at x_i is given by $A(\kappa_j(x_i), x_i)e^{i\phi_0(x_i)}$. Therefore, the probability amplitude for the two particles to be produced at the source points, to propagate from the source points to the freeze-out points, and to arrive at the detection points is

$$A(\kappa_1(x_1), x_1)e^{i\phi_0(x_1)}A(\kappa_2(x_2), x_2)e^{i\phi_0(x_2)} \exp\{-i \int_{x_1}^{x_{f1}} \kappa_1(x') \cdot dx' - ik_1 \cdot (x_{d1} - x_{f1})\} \\ \times \exp\{-i \int_{x_2}^{x_{f2}} \kappa_2(x') \cdot dx' - ik_2 \cdot (x_{d2} - x_{f2})\}. \quad (18)$$

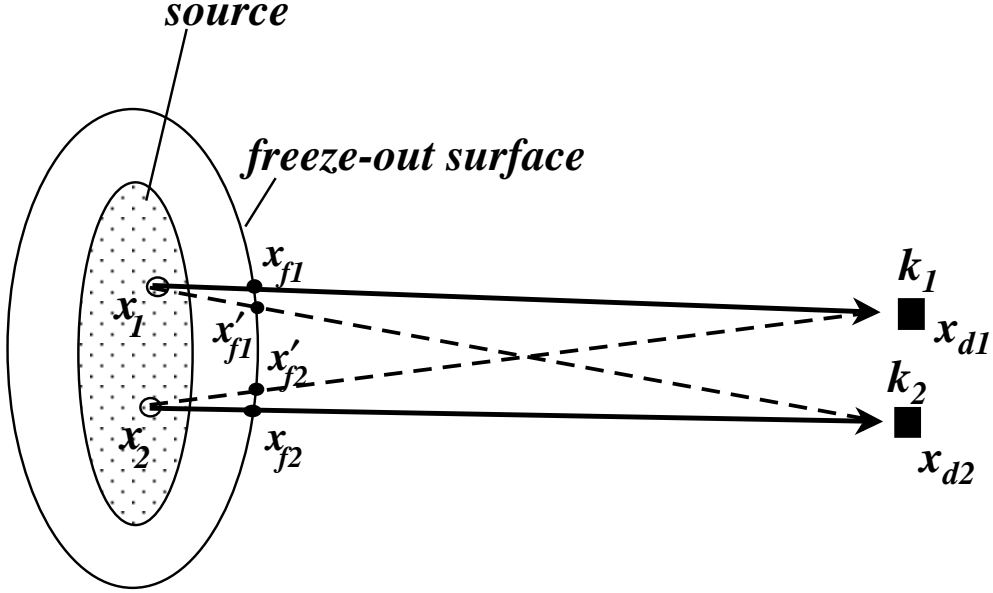


FIG. 2: A particle of momentum k_1 is detected at x_{d1} and another identical particle with momentum k_2 is detected at the space-time point x_{d2} . They are emitted from the source point x_1 and x_2 of an extended source. The solid lines joining $x_1 \rightarrow x_{f1} \rightarrow x_{d1}$ for k_1 and $x_2 \rightarrow x_{f2} \rightarrow x_{d2}$ for k_2 , and the dashed lines joining $x_1 \rightarrow x'_{f1} \rightarrow x_{d2}$ for k_2 and $x_2 \rightarrow x'_{f2} \rightarrow x_{d1}$ for k_1 are possible trajectories.

However, this is not the only probability amplitude contribution for two identical particles produced from x_1 and x_2 to arrive at x_{d1} and x_{d2} . The particle of momentum k_1 detected at x_{d1} can also be produced at x_2 with momentum $\kappa_1(x_2)$, propagate from x_2 to the freeze-out point $x'_{f2}(x_2)$, and arrives at x_{d1} with momentum k_1 , while the other identical particle of momentum $\kappa_2(x_1)$ starts at x_1 , propagates from x_1 to the freeze-out point $x'_{f1}(x_1)$, and arrives at x_{d2} with momentum k_2 , as indicated by the dashed lines in Fig. 2. As the distances between the freeze-out points and the source points are much smaller than the distances between the freeze-out points, and the detection points and two-particle correlations occur for k_1 close to k_2 , it is reasonable to make the approximations $x'_{f1} = x_{f1}$ and $x_{f2} = x'_{f2}$ (see Fig. 2). The probability amplitude for this occurrence along the trajectories $x_1 \rightarrow x'_{f1} \rightarrow x_{d2}$ for k_2 and $x_2 \rightarrow x'_{f2} \rightarrow x_{d1}$ for k_1 is

$$\begin{aligned}
& A(\kappa_1(x_2), x_2) e^{i\phi_0(x_2)} A(\kappa_2(x_1), x_1) e^{i\phi_0(x_1)} \exp\{-i \int_{x_2}^{x_{f2}} \kappa_1(x') \cdot dx' - ik_1 \cdot (x_{d1} - x_{f2})\} \\
& \times \exp\{-i \int_{x_1}^{x_{f1}} \kappa_2(x') \cdot dx' - ik_2 \cdot (x_{d2} - x_{f1})\}. \quad (19)
\end{aligned}$$

Because of the indistinguishability of the particles and the Bose-Einstein statistics of iden-

tical bosons (or the Fermi-Dirac statistics for fermions), the probability amplitude must be symmetrical (or antisymmetrical) with respect to the interchange of the labels of the particles which distinguish them. In this case, the only labels which distinguish the two identical particles are the source point coordinates x_1 and x_2 , because one particle of momentum k_1 has been determined to have been detected at x_{d1} and the other identical particle of momentum k_2 at x_{d2} . The probability amplitude must be symmetrical for bosons and anti-symmetrical for fermions, with respect to the interchange of the labels x_1 and x_2 . Accordingly, the probability amplitude which satisfies this symmetry is the sum (or difference) of Eqs. (18) and (19) divided by $\sqrt{2}$:

$$\begin{aligned} & \frac{1}{\sqrt{2}} \left\{ A(\kappa_1(x_1), x_1) e^{i\phi_0(x_1)} A(\kappa_2(x_2), x_2) e^{i\phi_0(x_2)} \exp\left\{-i \int_{x_1}^{x_{f1}} \kappa_1(x') \cdot dx' - ik_1 \cdot (x_{d1} - x_{f1})\right\} \right. \\ & \quad \times \exp\left\{-i \int_{x_2}^{x_{f2}} \kappa_2(x') \cdot dx' - ik_2 \cdot (x_{d2} - x_{f2})\right\} \\ & \quad + \theta A(\kappa_1(x_2), x_2) e^{i\phi_0(x_2)} A(\kappa_2(x_1), x_1) e^{i\phi_0(x_1)} \exp\left\{-i \int_{x_2}^{x_{f2}} \kappa_1(x') \cdot dx' - ik_1 \cdot (x_{d1} - x_{f2})\right\} \\ & \quad \times \exp\left\{-i \int_{x_1}^{x_{f1}} \kappa_2(x') \cdot dx' - ik_2 \cdot (x_{d2} - x_{f1})\right\} \left. \right\} \\ & \equiv e^{i\phi_0(x_1)} e^{i\phi_0(x_2)} \Phi(\kappa_1 \kappa_2, x_1 x_2 \rightarrow x_{d1} x_{d2}), \end{aligned} \quad (20)$$

where θ is 1 for bosons, -1 for fermions, and $\Phi(\kappa_1 \kappa_2, x_1 x_2 \rightarrow x_{d1} x_{d2})$ is the part of the probability amplitude in the above equation which does not depend on ϕ_0 . It is defined by

$$\begin{aligned} & \Phi(\kappa_1 \kappa_2 : x_1 x_2 \rightarrow x_{d1} x_{d2}) \\ & = \frac{1}{\sqrt{2}} \left\{ A(\kappa_1(x_1), x_1) A(\kappa_2(x_2), x_2) \exp\left\{-i \int_{x_1}^{x_{f1}} \kappa_1(x') \cdot dx' - ik_1 \cdot (x_{d1} - x_{f1})\right\} \right. \\ & \quad \times \exp\left\{-i \int_{x_2}^{x_{f2}} \kappa_2(x') \cdot dx' - ik_2 \cdot (x_{d2} - x_{f2})\right\} \\ & \quad + \theta A(\kappa_1(x_2), x_2) A(\kappa_2(x_1), x_1) \exp\left\{-i \int_{x_2}^{x_{f2}} \kappa_1(x') \cdot dx' - ik_1 \cdot (x_{d1} - x_{f2})\right\} \\ & \quad \times \exp\left\{-i \int_{x_1}^{x_{f1}} \kappa_2(x') \cdot dx' - ik_2 \cdot (x_{d2} - x_{f1})\right\} \left. \right\}. \end{aligned} \quad (21)$$

Besides originating from the source points x_1 and x_2 , the two particles can also be produced at other source points in the extended source. The total amplitude is the sum of amplitudes from all combinations of two source points. Therefore, the total probability amplitude for two identical particles to be produced from two source points in the extended source and to arrive at their respective detection points x_{d1} and x_{d2} with momenta k_1 and k_2 is

$$\begin{aligned} \Psi(k_1 k_2 : \{\text{all } x_1 x_2\}_{\text{points}} \rightarrow x_{d1} x_{d2}) & = \sum_{\{x_1, x_2\}} e^{i\phi_0(x_1)} e^{i\phi_0(x_2)} \left[\Phi(\kappa_1 \kappa_2 : x_1 x_2 \rightarrow x_{d1} x_{d2}) \right. \\ & \quad \left. + \theta \Phi(\kappa_1 \kappa_2 : x_2 x_1 \rightarrow x_{d1} x_{d2}) \right] \end{aligned} \quad (22)$$

where the sum is carried over distinct combinations of $\{x_1, x_2\}$. The two-particle momentum distribution $P(k_1, k_2)$ is defined as the probability distribution for two particles of momenta k_1 and k_2 to be produced from the extended source and to arrive at their respective detection points x_{d1} and x_{d2} . From Eq. (22), it is given by

$$P(k_1, k_2) = \frac{1}{2!} |\Psi(\kappa_1 \kappa_2 : \{\text{all } x_1 x_2\} \rightarrow x_{d1} x_{d2})|^2. \quad (23)$$

We now apply the results of Eqs. (21)-(23) to examine the momentum correlations of a chaotic source. A chaotic source is described by a phase function $\phi_0(x)$ that is a random and fluctuating function of the source point coordinate x . For a chaotic source, we again make use of the random and fluctuating nature of the phases by substituting Eq. (21) into Eq. (22) and expand the righthand side of Eq. (23). We separate out terms which are independent of ϕ_0 and terms which contain ϕ_0 . We obtain

$$\begin{aligned} P(k_1, k_2) = & \frac{1}{2} \sum_{x_1, x_2} \left\{ \Phi^*(\kappa_1 \kappa_2 : y_1 y_2 \rightarrow x_{d1} x_{d2}) \Big|_{\substack{y_1=x_1 \\ y_2=x_2}} \Phi(\kappa_1 \kappa_2 : x_1 x_2 \rightarrow x_{d1} x_{d2}) \right. \\ & \left. + \theta \Phi^*(\kappa_1 \kappa_2 : y_1 y_2 \rightarrow x_{d1} x_{d2}) \Big|_{\substack{y_2=x_1 \\ y_1=x_2}} \Phi(\kappa_1 \kappa_2 : x_1 x_2 \rightarrow x_{d1} x_{d2}) \right\} \\ & + \frac{1}{2} \sum_{\substack{x_1, x_2, y_1, y_2 \\ \{x_1 x_2\} \neq \{y_1 y_2\}}} \left\{ e^{i\phi_0(x_1) + i\phi_0(x_2) - i\phi_0(y_1) - i\phi_0(y_2)} \right. \\ & \left. \times \Phi^*(\kappa_1 \kappa_2 : y_1 y_2 \rightarrow x_{d1} x_{d2}) \Phi(\kappa_1 \kappa_2 : x_1 x_2 \rightarrow x_{d1} x_{d2}) \right\}. \quad (24) \end{aligned}$$

The two terms in the first summation on the righthand side are equal because of exchange symmetry. For the chaotic source, the last term in Eq. (24) gives a zero sum because the contributions of a large number of terms with similar magnitudes but random and fluctuating phases cancel out. Therefore, Eq. (24) becomes

$$P(k_1, k_2) = \sum_{x_1, x_2} |\Phi(\kappa_1 \kappa_2 : x_1 x_2 \rightarrow x_{d1} x_{d2})|^2, \quad (25)$$

Converting the summations in Eq. (25) into integrals with the transcription (12), we can rewrite the total probability as a double integral over the source point coordinates x_1 and x_2 ,

$$P(k_1, k_2) = \int d^4 x_1 d^4 x_2 \rho(x_1) \rho(x_2) |\Phi(\kappa_1 \kappa_2 : x_1 x_2 \rightarrow x_{d1} x_{d2})|^2. \quad (26)$$

In the above equation, $|\Phi|^2$ can be obtained by using Eq. (21). We get

$$|\Phi|^2 = A^2(\kappa_1(x_1), x_1)A^2(\kappa_2(x_2), x_2) + \theta A(\kappa_1(x_1), x_1)A(\kappa_2(x_2), x_2)A(\kappa_1(x_2), x_2)A(\kappa_2(x_1), x_1)) \frac{e^{i(A+B)} + e^{-i(A+B)}}{2}, \quad (27)$$

where

$$\begin{aligned} \mathcal{A} &= -\int_{x_1}^{x_{f1}} \kappa_1(x') \cdot dx' - \int_{x_2}^{x_{f2}} \kappa_2(x') \cdot dx' + \int_{x_1}^{x_{f1}} \kappa_2(x') \cdot dx' + \int_{x_2}^{x_{f2}} \kappa_1(x') \cdot dx' \\ &= -\int_{x_1}^{x_{f1}} [\kappa_1(x') - \kappa_2(x')] \cdot dx' - \int_{x_2}^{x_{f2}} [\kappa_2(x') - \kappa_1(x')] \cdot dx', \end{aligned} \quad (28)$$

and

$$\begin{aligned} \mathcal{B} &= k_1 \cdot (x_{f1} - x_{d1}) + k_2 \cdot (x_{f2} - x_{d2}) - k_1 \cdot (x_{f2} - x_{d1}) - k_2 \cdot (x_{f1} - x_{d2}) \\ &= (k_1 - k_2) \cdot x_{f1} + (k_2 - k_1) \cdot x_{f2}. \end{aligned} \quad (29)$$

Therefore, we have

$$\begin{aligned} P(k_1, k_2) &= \int d^4x_1 \rho(x_1) A^2(\kappa_1(x_1), x_1) \int d^4x_2 \rho(x_2) A^2(\kappa_2(x_2), x_2) \\ &+ \theta \int d^4x_1 \rho(x_1) A(\kappa_1(x_1), x_1) A(\kappa_2(x_1), x_1) e^{i(k_1 - k_2) \cdot x_1} \exp\{-i \int_{x_1}^{x_{f1}} \{[\kappa_1(x') - \kappa_2(x')] - [k_1 - k_2]\} \cdot dx'\} \\ &\times \int d^4x_2 \rho(x_2) A(\kappa_2(x_2), x_2) A(\kappa_1(x_2), x_2) e^{-i(k_1 - k_2) \cdot x_2} \exp\{-i \int_{x_2}^{x_{f2}} \{[\kappa_1(x') - \kappa_2(x')] - [k_1 - k_2]\} \cdot dx'\} \end{aligned} \quad (30)$$

Using Eq. (13), we can rewrite the above equation as

$$\begin{aligned} P(k_1, k_2) &= P(k_1)P(k_2) \\ &+ \theta \left| \int d^4x e^{i(k_1 - k_2) \cdot x} \exp\{-i \int_x^{x_f} \{[\kappa_1(x') - \kappa_2(x')] - [k_1 - k_2]\} \cdot dx'\} \rho(x) A(\kappa_1(x), x) A(\kappa_2(x), x) \right|^2, \end{aligned} \quad (31)$$

which is independent of x_d . It is convenient to rewrite the two-particle distribution function as

$$P(k_1, k_2) = P(k_1)P(k_2) \left(1 + \theta \left| \int d^4x e^{i(k_1 - k_2) \cdot x + i\phi_c(x, k_1 k_2)} \rho_{\text{eff}}(x; k_1 k_2) \right|^2 \right), \quad (32)$$

where ρ_{eff} is the effective density

$$\rho_{\text{eff}}(x; k_1 k_2) = \frac{\rho(x) A(\kappa_1(x), x) A(\kappa_2(x), x)}{\sqrt{P(k_1)P(k_2)}}, \quad (33)$$

and $\phi_c(x, k_1 k_2)$ is the collective flow phase function

$$\phi_c(x, k_1 k_2) = - \int_x^{x_f} \{[\kappa_1(x') - \kappa_2(x')] - [k_1 - k_2]\} \cdot dx' . \quad (34)$$

The HBT two-particle correlation function $R(k_1, k_2) = P(k_1, k_2)/P(k_1)P(k_2) - 1$ becomes

$$R(k_1, k_2) = \theta \left| \int d^4x e^{i(k_1 - k_2) \cdot x + i\phi_c(x, k_1 k_2)} \rho_{\text{eff}}(x; k_1 k_2) \right|^2 . \quad (35)$$

From Eq. (5), we have

$$[\kappa_1(x') - \kappa_2(x')] - [k_1 - k_2] = [\Lambda(\boldsymbol{\beta}(x')) - \Lambda(\boldsymbol{\beta}(x_f))] \Lambda^{-1}(\boldsymbol{\beta}(x_f))(k_1 - k_2) . \quad (36)$$

The collective flow phase $\phi_c(x, k_1 k_2)$ becomes

$$\phi_c(x, k_1 k_2) = - \int_x^{x_f} dx' \cdot \{[\Lambda(\boldsymbol{\beta}(x')) - \Lambda(\boldsymbol{\beta}(x_f))] \Lambda^{-1}(\boldsymbol{\beta}(x_f))(k_1 - k_2)\} . \quad (37)$$

Thus, under a collective flow the two-particle correlation function depends on the initial source distribution and a collective flow phase function $\phi_c(x, k_1 k_2)$, as given by Eqs. (32)-(35). When there is no collective flow, $\phi_c(x, k_1 k_2)$ is zero, and $P(k_1, k_2)$ and $R(k_1, k_2)$ reduce to the usual two-particle correlation functions of Eqs. (17.29) and (17.38) in Ref. [2].

We note that the collective flow phase function $\phi_c(x, k_1 k_2)$ consists of the differences $\Lambda(\boldsymbol{\beta}(x')) - \Lambda(\boldsymbol{\beta}(x_f))$ and $k_1 - k_2$ which can lead to substantial cancellation. In fact, if $\boldsymbol{\beta}(x')$ reaches the asymptotic velocity $\boldsymbol{\beta}(x_f)$, then there will be no contribution from this path element dx' at x' to the phase function $\phi_c(x, k_1 k_2)$.

The velocity profile $\boldsymbol{\beta}(x')$ of a source can be obtained by solving the relativistic hydrodynamical equations. We can get some ideas on the expansion scenario for a highly compressed relativistic ideal fluid initial at rest from the results of Rischke and Gyulassy [33]. We can consider a spherical fireball in which the collective flow is along the radial direction. (The transverse expansion of a Bjorken cylinder can be discussed in a similar way [33].) When this highly compressed fluid is allowed to evolve hydrodynamically, fluid elements at the surface reach their asymptotic velocity (close to the speed of light) very rapidly — nearly at the beginning of the expansion. Fluid elements at the central region remain essentially at rest until they are carried outward by the strong rebounding wave, and they reach the asymptotic velocity also rapidly.

From Fig. 2 of [33], the velocity of the fluid element initial at (r, θ, ϕ) is approximately

$$\boldsymbol{\beta}(x') = \boldsymbol{\beta}(x_c) \theta(t' - t_c) \quad \text{for } t \leq t' \leq t_c \quad (38)$$

where $t_c = t + 2(R - r)$, $r \leq R$, and R is the radius of the initial source. The trajectory for the fluid element is $r'(t') = r + \beta(x')t'$, $\theta'(t') = \theta$, and $\phi'(t') = \phi$. For such a collective flow, we can describe this as an initial source up to $t = t_c$, and the source undergoes collective flow at $t > t_c$ with a flow velocity reaching the asymptotic velocity approximately in a step-wise manner. Fluid elements reaching the asymptotic velocity do not contribute to the collective phase $\phi_c(x, k_1 k_2)$, as one notes previously in Eq. (37). The collective flow phase function $\phi_c(x, k_1 k_2)$ is approximately zero for this case. For other initial conditions and compression, the radial expansion and rapid rise of the collective velocity to the asymptotic velocity should be similar, as the collective motion arises from the expansion of a compressed matter into an empty vacuum. The magnitude of the asymptotic velocity may depend on the degree of compression (and therefore on the heavy-ion collision energy). The collective flow phase function ϕ_c will likely remain small because of the substantial cancellation in Eq. (37) mentioned above. We should expect that the effective density measured in HBT measurements should depend essentially on the initial source distribution. Much more work will be required to examine further the behavior of $\phi_c(x, k_1 k_2)$ and $R(k_1 k_2)$ for general flows and initial conditions.

IV. EFFECTS OF MULTIPLE SCATTERING AND OPTICAL POTENTIAL

The observation of the intensity interferometry depends on the degree of coherence or chaoticity of the source. As the initial source particles traverse from the source point x_i to the freeze-out point x_{fi} under a collective flow, they are subject to multiple scattering with medium particles. One may think that as a result of these scatterings, the source becomes chaotic at freeze-out and the distribution observed in an HBT measurement should correspond to the freeze-out distribution [5, 24].

The problem of multiple scattering must however be treated properly in the context of intensity interferometry. As the Hanbury-Brown-Twiss effect is purely a quantum-mechanical effect, the problem of multiple scattering must be investigated within the quantum-mechanical framework in terms of probability amplitudes instead of incoherent collisions involving probabilities and cross sections.

Within such a theoretical framework, we can study our problem in the Glauber model [44, 45] or the optical model [47, 48, 49, 50, 51, 52], depending on the energy of the detected

particle relative to the medium. The Glauber theory has been applied successfully to study the interaction of a pion with the nuclear medium at a pion energy from 300 to 1200 MeV [45, 46, 47]. It can therefore be used to study the interaction of an energetic pion with the hadron medium produced in high-energy heavy-ion collisions. At these energies, the trajectory can be approximately described as a straight line, the probability amplitude for the particle to traverse from x to x' after suffering multiple scatterings with particles in the medium is

$$\exp\{i\phi_s(x \rightarrow x')\} = \exp\left\{i \sum_{j=2}^N \chi(\mathbf{x}'_{\perp} - \mathbf{s}_{j\perp})\theta(\mathbf{x}'_{\parallel} - \mathbf{s}_{j\parallel})\theta(\mathbf{s}_{j\parallel} - \mathbf{x}_{\parallel})\right\}, \quad (39)$$

where the function $\chi(\mathbf{x}'_{\perp} - \mathbf{s}_{j\perp})$ is the Glauber phase shift function for the interaction of the produced particle with a medium particle at \mathbf{s}_j and the sum \sum_j is carried over all medium particles having coordinates $x_j = (t_j, \mathbf{s}_{j\parallel}, \mathbf{s}_{j\perp}), j = 2, 3, \dots, N$ [44]. The phase shift function $\chi(\mathbf{b})$ can be obtained from two-body scattering data and is an analytical function of the transverse coordinate \mathbf{b} . The subscript \perp in Eq. (39) denotes the component transverse to the particle trajectory and the subscript \parallel denotes the component along the trajectory.

The wave function Eq. (39) from Glauber multiple scattering theory contains a wealth of relevant information. It depends on the coordinates of all the particles with which the incident particle has interacted. It treats correctly the case of no scattering and multiple scattering, even up to the extreme case of $N - 1$ scatterings in succession. It makes no difference whether the medium particles are dense in close proximity or dilute in far separation. Information on the density of medium particles can be provided when one integrates out the distribution of the medium particles.

One can show that starting with the multiple scattering wave function Eq. (39), one can construct the Wigner function in the transverse and longitudinal degrees of freedom. The multiple scattering wave function Eq. (39) leads naturally to the diffractive transport theory, and the equation of motion for the Wigner function is just the Boltzmann equation [54]. The solution of the Wigner function can be decomposed into multiple-scattering components each of which corresponds to the scattering of the incident particle with a definite number of medium particles. The transverse width of the n -scattering component increases with \sqrt{n} and the maximum of the longitudinal distribution of the n -scattering component is located longitudinally at n times the mean-free path.

As Glauber multiple scattering theory gives the classical diffractive transport theory on

the one hand, and retains the wave nature of the propagation on the other hand, it is therefore appropriate to use Glauber multiple scattering wave function to investigate the effects of multiple scattering in intensity interferometry.

Using this description for the multiple scattering of the particle, the probability amplitude for the produced particle to travel from the source point x to x_d becomes

$$\Psi(\kappa x \rightarrow k x_d) = A(\kappa x) e^{i\phi(x)} \psi(\kappa x \rightarrow k x_d) \quad (40)$$

where $\phi(x)$ is

$$\phi(x) = \phi_0(x) + \phi_s(x \rightarrow x_f), \quad (41)$$

$\phi_0(x)$ is the initial random and fluctuating phase due to the chaoticity of the production source, and $\phi_s(x \rightarrow x_f)$ is

$$\phi_s(x \rightarrow x_f) = \sum_{j=2}^N \chi(\mathbf{x}_{f\perp} - \mathbf{s}_{j\perp}) \theta(\mathbf{x}_{f\parallel} - \mathbf{s}_{j\parallel}) \theta(\mathbf{s}_{j\parallel} - \mathbf{x}_{\parallel}). \quad (42)$$

As x_f is a function of x , the phase function $\phi_s(x \rightarrow x_f)$ is a function of x and can be abbreviated as $\phi_s(x)$. It contains a real and imaginary part. The imaginary part is given by

$$\mathcal{I}m \phi_s(x) = \sum_{j=2}^N \mathcal{I}m \chi(\mathbf{x}_{f\perp} - \mathbf{s}_{j\perp}) \theta(\mathbf{x}_{f\parallel} - \mathbf{s}_{j\parallel}) \theta(\mathbf{s}_{j\parallel} - \mathbf{x}_{\parallel}), \quad (43)$$

and it represents the degree of absorption as the detected particle passes through the medium.

With this modification, the derivation of the single-particle and two-particle distributions can be carried out as in the last sections. As the multiple scattering bring in a complex phase $\phi_s(x)$ that depends on x , the quantum description of the scattering amplitude leads to the single-particle distribution

$$P(k) = \int dx_2 dx_3 dx_4 \dots dx_N \sum_x e^{i(\phi_s(x) - \phi_s^*(x))} A^2(\kappa(x), x) \rho_{\text{med}}(x_2, x_3, x_4, \dots, x_N), \quad (44)$$

where $\rho_{\text{med}}(x_2, x_3, x_4, \dots, x_N)$ is the distribution of the medium particles. Note that the real part of $\phi_s(x)$ cancel out in the factor $\phi_s(x) - \phi_s^*(x)$ in the above equation. Consequently, when the multiple scattering between the detected particle and the medium is taken into account, the single-particle distribution for a collective flow is

$$P(k) = \int d^4x e^{-2 \mathcal{I}m \bar{\phi}_s(x)} \rho(x) A^2(\kappa(x), x), \quad (45)$$

where

$$e^{-2 \mathcal{I}m \bar{\phi}_s(x)} = \int dx_2 dx_3 dx_4 \dots dx_N e^{-2 \mathcal{I}m \phi_s(x)} \rho_{\text{med}}(x_2, x_3, x_4, \dots, x_N). \quad (46)$$

In this case, we have

$$P(k) = \int d^4x f_{\text{init}}(\kappa(x), x), \quad (47)$$

where

$$f_{\text{init}}(\kappa(x), x) = e^{-2 \mathcal{I}m \bar{\phi}_s(x)} \rho(x) A^2(\kappa(x), x). \quad (48)$$

The two-particle distribution for a system with a collective flow can be obtained as in the last section, and we get

$$P(k_1, k_2) = P(k_1)P(k_2) + \theta \left| \int d^4x e^{i(k_1 - k_2) \cdot x + i\phi_c(x, k_1 k_2)} e^{-2 \mathcal{I}m \bar{\phi}_s(x)} \rho(x) A(\kappa_1(x), x) A(\kappa_2(x), x) \right|^2, \quad (49)$$

or

$$P(k_1, k_2) = P(k_1)P(k_2) \left(1 + \theta \left| \int d^4x e^{i(k_1 - k_2) \cdot x + i\phi_c(x, k_1 k_2)} e^{-2 \mathcal{I}m \bar{\phi}_s(x)} \rho_{\text{eff}}(x; k_1 k_2) \right|^2 \right), \quad (50)$$

where $\phi_c(x, k_1 k_2)$ is given by Eq. (34) and $\rho_{\text{eff}}(x; k_1 k_2)$ is given by Eq. (33). Thus, multiple scattering leads to an absorption of produced particles as they traverse from the source point to the freeze-out point. There is an absorption factor in both the single-particle distribution and the two-particle correlation function. The effective density distribution ρ_{eff} revealed by HBT two-particle correlation measurements depends on the initial source distribution and not necessarily on the freeze-out density distribution.

At lower energies, the interaction of the pion with the medium can be described by an optical model [47, 48, 49, 50, 51, 52]. For example, in the interaction of a pion with a nucleus, a local phenomenological optical potential has been successfully applied to explain the π -nucleus elastic scattering data from 120 MeV to 766 MeV [48, 49, 50]. The effects of intermediate resonances such as $\Delta(1232)$ shows up as giving rise to a peak in the imaginary part of the optical potential near the $\Delta(1323)$ resonance energy. The optical potential is normally non-local but can be described in terms of a local-equivalent potential by redefining some kinematic quantities [48]. A ‘‘model-exact’’ microscopic description of the optical potential has also been developed to describe the interaction of a pion with a nuclear medium

in terms of the interaction between the pion and medium particles, including the effects of the $\Delta(1323)$, $\Delta_{13}(1520)$, and $F_{15}(1680)$ resonances [51, 52].

Based on the successes of the optical model in describing the interaction between a pion and nuclear matter, it is reasonable to use similar descriptions to study the dynamics of an intermediate-energy pion in hadronic matter produced in high-energy heavy-ion collisions. An optical model is specially appropriate as the Hanbury-Brown-Twiss intensity interferometry arises from an optical interference of the wave amplitudes.

One can accordingly introduce a complex optical potential $V(k, x)$ with a negative imaginary part to describe the interaction between the detected particle and the medium particles as it travels from the source point to the freeze-out point. The optical potential V depends on the momentum of the particle k . The momentum dependence is particularly pronounced in the neighborhood of a resonance. In principle, the optical potential can be determined from two-body data and the distribution of particles in the medium, as carried out for example in Ref. [47, 51, 52]. Under the interaction of an optical potential $V(k, x)$, the amplitude for a produced particle to propagate from x to x'' is given by [44]

$$\exp\{i\phi_s(x \rightarrow x'')\} = \exp\{-i \int_x^{x''} \frac{1}{v} V(k, x') dx'_{\parallel}\}, \quad (51)$$

where v is the magnitude of the velocity of the detected particle relative to the hadron medium along the direction of propagation. Therefore, when the multiple scattering between x and x_f is taken into account, the probability amplitude for the particle to propagate from x to x_d becomes

$$\Psi(\kappa x \rightarrow \kappa x_d) = A(\kappa x) e^{i\phi(x)} \psi(\kappa x \rightarrow \kappa x_d), \quad (52)$$

where

$$\phi(x) = \phi_0(x) - \int_x^{x_d} \frac{1}{v} V(k, x') dx'_{\parallel}. \quad (53)$$

The phase shift due to the optical potential, $\phi_s(k, x)$, is a complex quantity containing a real and an imaginary part,

$$\phi_s(k, x) = - \int_x^{x_f} \frac{1}{v} V(k, x') dx'_{\parallel}. \quad (54)$$

As x_f is a function of x , the phase function $\phi_s(x \rightarrow x_f)$ is a function of k and x and can be abbreviated as $\phi(k, x)$.

With this modification, the derivation of the single-particle and two-particle distributions can be carried out as in the case with the Glauber theory. The two-particle correlation function $R(k_1, k_2)$ becomes

$$R(k_1, k_2) = \left| \int d^4x e^{i(k_1 - k_2) \cdot x + i\phi_c(x, k_1 k_2)} e^{i(\phi_s(k_1, x) - \phi_s^*(k_2, x))} \rho_{\text{eff}}(x; k_1 k_2) \right|^2, \quad (55)$$

where

$$\mathcal{R}e(\phi_s(k_1, x) - \phi_s^*(k_2, x)) = - \int_x^{x_d} \left(\frac{1}{v_1} \mathcal{R}e V(k_1, x') dx'_{\parallel} - \frac{1}{v_2} \mathcal{R}e V(k_2, x') dx'_{\parallel} \right), \quad (56)$$

$$\begin{aligned} \mathcal{I}m(\phi_s(k_1, x) - \phi_s^*(k_2, x)) &= - \int_x^{x_d} \left(\frac{1}{v_1} \mathcal{I}m V(k_1, x') dx'_{\parallel} + \frac{1}{v_2} \mathcal{I}m V(k_2, x') dx'_{\parallel} \right) \\ &= 2\mathcal{I}m \bar{\phi}_s(x) \end{aligned} \quad (57)$$

and $v_i = |(\mathbf{k}_i)_{\parallel}|/k_i^0$. For low-energy detected particles, the velocities of the two detected particles can differ substantially and the real part of the phase function does not cancel exactly. There will be a substantial correction to the two-particle correlation function at low energies [26, 27]. For detected pions particles with kinetic energies close to or greater than its rest mass, in which we shall focus our attention, $v_i \sim 1$. The real parts of the phase function $\phi_s(k, x)$ cancel and there will be negligible modification of the two-particle correlation function. We again obtain the results of Eqs. (44), (45), and (48) for the single-particle distribution, and the result of Eq. (49) for the two-particle distribution.

In applying the Glauber theory at high energies or the optical model at intermediate energies, the precise energy at which one needs to switch from the Glauber theory to the optical model needs not concern us here at present as both descriptions lead to a complex phase shift function $\phi_s(x)$. The imaginary part of the phase shift function gives rise to an absorption. The real part of the phase shift leads to negligible modification of the two-particle correlation function. The conclusion concerning the real phase of coordinate is a rather general result. Any final-state interaction, that leads to an additional real phase function of coordinate and a weak dependence on momentum, does not modify the two-particle correlation. As a consequence, the effective density distribution depends on the initial source distribution and not necessarily on the freeze-out distribution. The intensity interferometry arises from the difference in the phases when the two particles takes on two different sets of histories. For either set of histories depicted in Fig. 2, even though the amplitude for the propagation from x_1 to x_2 depends on the positions of the medium

scatterer which can be random, the real parts of the phases in propagating from the source point to the freeze-out points are the same. They cancel out when we evaluate the HBT two-particle correlation function $R(k_1, k_2)$.

Previously, Gyulassy *et al.* found that the two-particle correlation function for a coherent source is unaffected by a final-state mean-field potential. For a chaotic source, which is the object of our interest here, they expressed the two-particle correlation function in terms of distorted waves in the mean-field [Eq. (5.32) of [7]]. The present results for the optical potential corresponds to an explicit evaluation of this two-particle correlation function using the eikonal approximation for high-energy particles. In the process of this evaluation, we find that the phase distortion due to a real mean-field potential cancels out, as we remarked earlier, and lead to negligible effect on the two-particle correlation at high particle energies. The distortions can however be substantial for low-energy particles as discussed in [26, 27].

V. CONCLUSIONS AND DISCUSSIONS

We start from the probability amplitude written in terms of the path integral over the classical trajectory for a single particle and a pair of identical particles. The sum over the probability amplitudes for a chaotic source leads to an intensity interference for the detection of two identical particles.

As the detected particles traverse from the source point to the freeze-out point, they are subject to scattering with particles in the medium. We have examined the effects of multiple scattering. Because the Hanbury-Brown-Twiss intensity interferometry is purely a quantum-mechanical phenomenon, we investigate the problem of multiple scattering within the quantum-mechanical framework of the Glauber theory and the optical model. We find that multiple scattering leads to an effective density distribution that depends on the initial source distribution rather than the freeze-out density distribution. This conclusion follows from the wave nature of the detected particle, which is an important ingredient for the occurrence of intensity interferometry. The Glauber multiple scattering amplitude and the optical model scattering also represent coherent scattering processes [44] as the corresponding phase function is an analytical function of the coordinate. There is the expected absorption arising from the imaginary part of the phase shift function in the multiple scattering process.

We have studied the multiple scattering process at high energies using the Glauber model

and at intermediate energies using the optical model in the eikonal approximation. At low energies when these simple approximations may not be valid, it will be of great interest to study a quantum mechanical description of the multiple scattering process using either a quantum mechanical many-particle theory or a pion mean-field optical potential without the eikonal approximation.

In the presence of a collective flow, we find that two-particle correlation measurements lead to an effective source distribution that depends on the initial source distribution. The relevant momentum is the initial momentum shifted from the detected momentum downward by the collective flow, as given by Eq. (33) obtained here. In addition, the collective flow leads to a phase function $\phi_c(x, k_1 k_2)$ in Eq. (34) which will modify the effective two-particle correlation. It consists of terms which tend to cancel each other. We examine sample results of hydrodynamical calculations of Rischke and Gyulassy [33] for a highly compressed relativistic fluid initially at rest. We find that the flow velocity of a fluid element reaches the asymptotic velocity rapidly at the surface, or in the interior when the rebounding wave carries the fluid element outward. There can be a substantial cancellation in the collective flow phase function $\phi_c(x, k_1 k_2)$. As a consequence, the effective density measured in HBT measurements is expected to depend essentially on the initial source distribution for such an expansion. Much more work will be required to examine further the behavior of $\phi_c(x, k_1 k_2)$ and $R(k_1, k_2)$ for general flows and initial conditions.

While further studies are continuing, it is interesting to explore the possibility that HBT measurements are indeed related mainly with the distribution of the initial source distribution. In that case, we expect that the initial source transverse dimension should be given approximately by the spatial dimension of the colliding nuclei which should be nearly independent of the collision energy. We also expect that in the initial source prior to the collective flow, the transverse size in the “out” direction should be approximately the same as that in the “side” direction. Hence, the HBT transverse radii should be approximately the same as the colliding nuclear radii, have only a weak collision-energy dependence, and $R_{\text{out}}/R_{\text{side}}$ should be approximately close to 1. These expectations are consistent with the gross features of HBT transverse radii in high-energy heavy-ion collisions [38, 39, 40, 41, 42, 43].

Acknowledgments

The author would like to thank Prof. R. Glauber for collaborative discussions on the multiple scattering model and diffractive transport. The author wishes to thank Drs. T. Awes, V. Cianciolo, M. Gyulassy, C. Pajares, S. Pratt, S. Sorensen, G. Young, and Weining Zhang for valuable discussions and comments. The author would like to thank specially Drs. T. Awes and V. Cianciolo for reading through the manuscript and making insightful suggestions. The author is indebted to Professor J. A. Wheeler for his earlier favorable comments on the treatment of intensity interferometry in author's book [2]. Professor Wheeler's comments provide additional impetus to investigate the present problem. This research was supported by the Division of Nuclear Physics, Department of Energy, under Contract No. DE-AC05-00OR22725 managed by UT-Battelle, LLC.

-
- [1] R. Hanbury-Brown and R. Q. Twiss, *Phil. Mag.* **45**, 633 (1954); R. Hanbury-Brown and R. Q. Twiss, *Phil. Mag. Nature* **177**, 27 (1956); R. Hanbury-Brown and R. Q. Twiss, *Phil. Mag. Nature* **178**, 1046, (1956).
 - [2] For a general review of the Hanbury-Brown-Twiss intensity interferometry, see Chapter 17 of C. Y. Wong, *Introduction to High-Energy Heavy-Ion Collisions*, World Scientific Publishing Company, 1994.
 - [3] W. Bauer, C. K. Gelke, and S. Pratt, *Ann. Rev. Nucl. Part. Sci.* **42**, 77 (1992).
 - [4] U. Heinz and B. Jacak, *Ann. Rev. Nucl. Part. Sci.* **49**, 529 (1992).
 - [5] U. A. Wiedemann, U. Heinz, *Phys. Rept.* 319 (1999) 145-230.
 - [6] R. J. Glauber, *Phys. Rev. Lett.* **10**, 84 (1963); R. J. Glauber, *Phys. Rev.* **130**, 2529 (1963); R. J. Glauber, *Phys. Rev.* **130**, 2766 (1963).
 - [7] M. Gyulassy, S. K. Kauffman, and L. W. Wilson, *Phys. Rev.* **C20**, 2267 (1979).
 - [8] D. Boal, C.-K. Gelbke, and B. K. Jennings, *Rev. Mod. Phys.* **62**, 553 (1990).
 - [9] W. A. Zajc, in *Particle Production in Highly Excited Matter*, Edited by H. H. Gutbrod and J. Rafelski, Plenum Press, New York, 1993, page 435.
 - [10] G. Goldhaber, S. Goldhaber, W. Lee, and A. Pais, *Phys. Rev.* **120**, 300 (1960).
 - [11] S. E. Koonin, *Phys. Lett.* **70B**, 43 (1977); F. B. Yano and S. E. Koonin, *Phys. Lett.* **B78**,

- 556 (1978).
- [12] G. I. Kopylov and M. J. Podgoretsky, *Yad. Fiz.* **18**, 656 (1973) [*Sov. J. Nucl. Phys.* **18**, 336 (1974)].
 - [13] G. N. Fowler and R. M. Weiner, *Phys. Lett.* **70B**, 201 (1977).
 - [14] S. Y. Fung, W. Gorn, G. P. Kiernan, J. J. Lu, Y. T. Oh, and R. T. Poe, *Phys. Rev. Lett.* **41**, 1592 (1978).
 - [15] M. Biyajima, *Phys. Lett.* **B92**, 193 (1980); M. Biyajima, *Prog. Theo. Phys.* **66**, 1378 (1981); M. Biyajima, *Prog. Theo. Phys.* **68**, 1273 (1982).
 - [16] S. Pratt, *Phys. Rev. Lett.* **53**, 1219 (1984).
 - [17] S. Pratt, *Phys. Rev.* **D33**, 72 (1986); S. Pratt, *Phys. Rev.* **D33**, 1314 (1986).
 - [18] Y. Hama and S. S. Padula, *Phys. Rev.* **D37**, 3237 (1988).
 - [19] C. C. Shih and P. Carruthers, *Phys. Rev.* **D38**, 56 (1988).
 - [20] M. Gyulassy and S. S. Padula, *Phys. Lett.* **B217**, 181 (1988).
 - [21] G. F. Bertsch, *Nucl. Phys.* **A498**, 173c (1989).
 - [22] Yu. M. Sinyukov, *Nucl. Phys.* **A498**, 151c (1989).
 - [23] V. Cianciolo, Ph. D. Thesis, M.I.T., 1994.
 - [24] U. A. Wiedemann, B. Tomášik, and U. Heinz, *Nucl. Phys.* **A638**, 475c (1998).
 - [25] A. Mikhlin and E. Surdutovich, *Phys. Rev.* **C59**, 2761 (1999).
 - [26] M.-C. Chu, S. Gardner, T. Matsui, and R. Seki, *Phys. Rev.* **C50**, 3079 (1994).
 - [27] T. D. Shoppa, S. E. Koonin, and R. Seki, *Phys. Rev.* **C61**, 054902 (2000).
 - [28] F. Grassi, Y. Hama, S. S. Padula, and O. Socolowski, Jr. *Phys. Rev.* **C62**, 044904 (2000).
 - [29] A. Ayala and A. Sánchez, *Phys. Rev.* **C63**, 044904 (2000).
 - [30] H. Nakamura and R. Seki, *Phys. Rev.* **C66**, 027901 (2002).
 - [31] M. A. Braun, F. del Moral, and C. Pajares, *Eur. Phys. J.* **C21**, 557 (2001); M. A. Braun, F. del Moral, and C. Pajares, *Phys. Lett.* **B551**, 291 (2003).
 - [32] W. N. Zhang, G. X. Tang, X. J. Chen, L. Huo, Y. M. Liu, and Z. Zhang, *Phys. Rev.* **C62**, 044903 (2000).
 - [33] D. H. Rischke and M. Gyulassy, *Nucl. Phys.* **A608**, 479 (1996).
 - [34] U. Heinz and P. Kolb, *Nucl. Phys.* **A702** (2002) 269-280.
 - [35] D. Zschesche, H. Stocker, W. Greiner, and S. Schramm, *Phys. Rev.* **C65**, 064902 (2002).
 - [36] D. Molnár and M. Gyulassy, *nucl-th/0204062*.

- [37] D. Molnár and M. Gyulassy, nucl-th/0211017.
- [38] K. Adcox *et al.*, PHENIX Collaboration, Phys. Rev. Lett. **88**, 192302 (2002).
- [39] C. Adler *et al.*, STAR Collaboration, Phys. Rev. Lett. **87**, 082302 (2001).
- [40] M. Lisa *et al.*, E895 Collaboration, Phys. Rev. Lett. **84**, 2789 (2000).
- [41] L. Ahle *et al.*, E802 Collaboration, Phys. Rev. **C66**, 054906 (2002);
- [42] I. G. Bearden *et al.*, NA44 Collaboration, Euro. Phys. Jour. **C18**, 317 (2000).
- [43] M.M. Aggarwal *et al.*, WA98 Collaboration, Eur. Phys. Jour. **C16**, 445 (2000).
- [44] R. J. Glauber, in *Lectures in Theoretical Physics*, edited by W. E. Brittin and L. G. Dunham (Interscience, N.Y., 1959), Vol. 1, p. 315.
- [45] M. Arima, K. Masutani, and R. Seki, Phys. Rev. **C44**, 415 (1991).
- [46] E. Oset, and D. Strottman, Phys. Rev. **C44**, 468 (1991).
- [47] M. B. Johnson and D. J. Ernst, Ann. Phys. (N.Y.) **219**, 266 (1992).
- [48] G. R. Satchler, Nucl. Phys. **A540**, 533 (1992).
- [49] M. B. Johnson and G. R. Satchler, Ann. Phys. (N.Y.), **248**, 134 (1996).
- [50] S. W. Hong and B. T. Kim, J. Phys. **G25**, 1065 (1999).
- [51] C. M. Chen, D. J. Ernst, and M. B. Johnson, Phys. Rev. **C48**, 841 (1993).
- [52] C. M. Chen, D. J. Ernst, M. F. Jiang, and M. B. Johnson, Phys. Rev. **C52**, R465 (1995).
- [53] M. Born and M. Wolf, *Principle of Optics*, Pergamon Press, 1964, New York.
- [54] C.Y. Wong and R. Glauber, to be published.